



## High-mobility *n*-channel organic field-effect transistors based on epitaxially grown C<sub>60</sub> films

Th.B. Singh<sup>a,\*</sup>, N. Marjanović<sup>a</sup>, G.J. Matt<sup>a</sup>, S. Günes<sup>a</sup>, N.S. Sariciftci<sup>a</sup>,  
A. Montaigne Ramil<sup>b</sup>, A. Andreev<sup>b</sup>, H. Sitter<sup>b</sup>, R. Schwödauer<sup>c</sup>, S. Bauer<sup>c</sup>

<sup>a</sup> Linz Institute for Organic Solar Cells (LIOS), Physical Chemistry, Johannes Kepler University Linz, Altenbergerstrasse 69, Linz A-4040, Austria

<sup>b</sup> Institute of Semiconductor and Solid State Physics, Johannes Kepler University Linz, Linz A-4040, Austria

<sup>c</sup> Soft Matter Physics, Johannes Kepler University Linz, Linz A-4040, Austria

Received 18 November 2004; received in revised form 9 March 2005; accepted 11 March 2005

Available online 19 April 2005

### Abstract

We present C<sub>60</sub>-based *n*-channel organic field-effect transistors with mobility in the range of 0.4–1 cm<sup>2</sup>V<sup>-1</sup>s<sup>-1</sup>. A solution-processed organic dielectric divinyltetramethyldisiloxane-bis(benzocyclobutene) (BCB) was used as a gate dielectric and C<sub>60</sub> films were grown on top by hot wall epitaxy. Devices characterised in inert atmosphere conditions show high stability with an on/off ratio >10<sup>4</sup>. The determined mobility values are nearly gate voltage independent.

© 2005 Elsevier B.V. All rights reserved.

### 1. Introduction

Organic thin-film electronics developed to a promising technology in the last two decades with demonstrated prototypes of organic thin film transistors, organic integrated circuits for radio frequency identification tags (RFID-tags) [1,2] and active matrix displays [3]. Organic field effect transistors (OFETs) have also been fabricated in arrays to drive electro-phoretic display pixels [4].

The performance of the individual transistors limits the switching speed in an integrated circuit, which can be roughly estimated by the ratio of mobility and channel length of the transistor [3]. To obtain higher switching speed, the search for higher mobility materials is therefore important along with the effort to downscale the transistor geometry.

Among all the various p-type organic semiconductors, pentacene in thin film form has been reported as promising material because of its mobility of 1.5 cm<sup>2</sup>V<sup>-1</sup>s<sup>-1</sup> [5a]. Organic single crystals such as rubrene have shown mobilities as high as 15 cm<sup>2</sup>V<sup>-1</sup>s<sup>-1</sup> [5b]. On the other hand,

\* Corresponding author. Tel.: +43 732 2468 8767; fax: +43 732 2468 8770.

E-mail address: [birendra.singh@jku.at](mailto:birendra.singh@jku.at) (Th.B. Singh).

very few organic semiconductors are n-type, viz., fullerenes, [6,7] fluorinated phthalocyanines, [8] naphthalenes and N-substituted naphthalene 1,4,5,8-tetracarboxylic diimide [9] or N,N'-dialkyl-3,4,9,10-perylene tetracarboxylic diimide (PTCDI, PTCDI-C<sub>5</sub> [10] and PTCDI-C<sub>8</sub>H, correspondingly) with a highest obtained mobility of  $0.6 \text{ cm}^2 \text{ V}^{-1} \text{ s}^{-1}$  [11]. Most of these results are achieved by growing the semiconductor on surface treated or untreated SiO<sub>2</sub> or Al<sub>2</sub>O<sub>3</sub>. Although the van der Waals type interactions between organic molecules and inorganic substrates are rather weak, the crystallographic phases, the orientation, and the morphology of the resulting organic semiconductor films critically depend on the interface and growth kinetics. In this paper, we present results on OFETs fabricated using hot wall epitaxy (HWE) grown C<sub>60</sub> films on top of an organic insulator. HWE, working close to thermodynamical

equilibrium is well known [12] as appropriate technique to grow highly ordered organic thin films, including C<sub>60</sub> films [13]. The relatively smooth surface of the organic insulating film interfaced with a highly ordered HWE grown C<sub>60</sub> film resulted in mobilities of  $0.4\text{--}1 \text{ cm}^2 \text{ V}^{-1} \text{ s}^{-1}$  and an on/off ratio  $>10^4$ . The obtained mobility is found to be nearly gate voltage independent with a normalised subthreshold slope of  $8 \text{ V nF/decade cm}^2$ . Furthermore, the field effect mobility has been found to be thermally activated with an activation energy of  $\sim 100 \text{ meV}$  within the temperature range of 90–300 K.

## 2. Experimental

A scheme of the device geometry is shown in Fig. 1(a). The device fabrication starts with etching

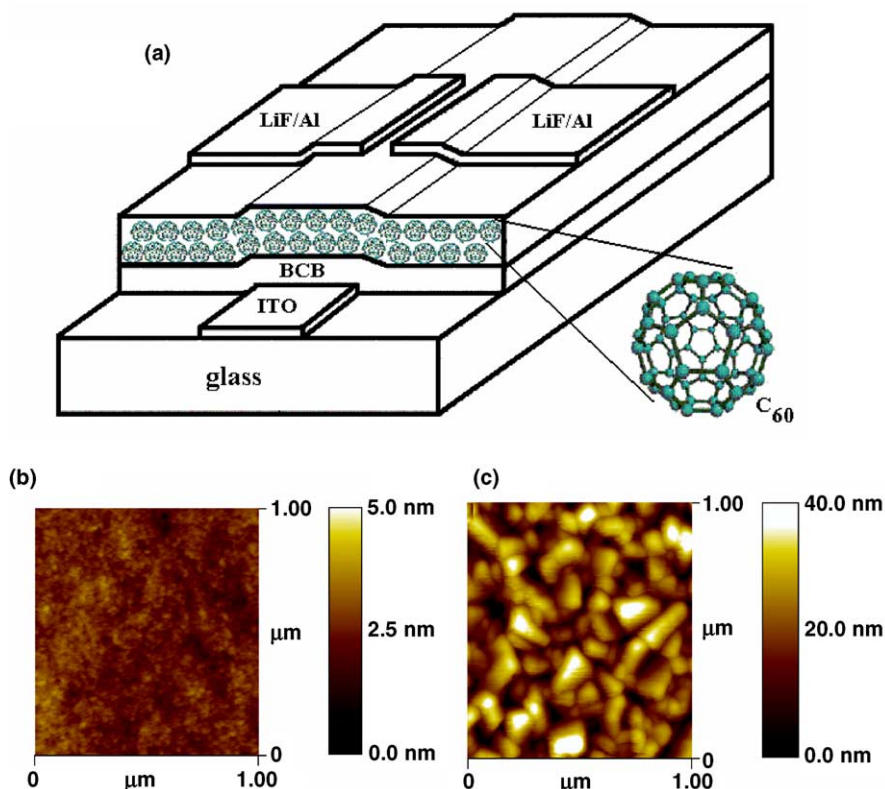


Fig. 1. (a) Scheme of the staggered *n*-channel OFET device structure; (b) AFM image of the BCB dielectric surface; (c) AFM image of the C<sub>60</sub> surface in the channel region of the fabricated OFET.

the indium tin oxide (ITO) on the glass substrate. After patterning the ITO and cleaning in an ultrasonic bath, a BCB layer is spin coated at 1500 rpm resulting in a 2  $\mu\text{m}$  thick film. BCB was used as received from Dow Chemicals and curing was done according to the standard procedure [14]. BCB is an excellent dielectric material with a rather low dielectric constant  $\epsilon_{\text{BCB}} = 2.6$  and a small, nearly temperature independent thermal expansion coefficient [15]. A 300 nm thick  $\text{C}_{60}$  film was grown by HWE on top of the dielectric at a substrate temperature of 130  $^{\circ}\text{C}$ . The top source and drain electrodes, (LiF/Al 0.6/60 nm) were evaporated under vacuum ( $2 \times 10^{-6}$  mbar) through a shadow mask. LiF/Al is expected to form ohmic contacts on fullerenes [16]. The channel length,  $L$  of the device is 35  $\mu\text{m}$  and the channel width is  $W = 1.4$  mm, which results in a  $W/L$  ratio of  $\approx 40$ . From the measurement of the BCB film thickness,  $d = 2$   $\mu\text{m}$  and the dielectric constant of BCB,  $\epsilon_{\text{BCB}} = 2.6$ , a dielectric capacitance  $C_{\text{BCB}} = 1.2$  nF/cm<sup>2</sup> was calculated. In our devices we have a  $d/L$  ratio  $\approx 0.05$  acceptable not to screen the gate field by the source drain contacts. Device transportation from the HWE chamber to the glove box and further electrical characterisation (using Keithley 236 and Keithley 2400 instruments) were carried out under argon environment. The surface morphology and thickness of the dielectric was determined with a Digital Instrument 3100 atomic force microscope (AFM) and a Dektak surface profilometer respectively. Device characterisation at various temperatures was performed in a He flow cryostat (Cryo Industries) using a Lakeshore 331 as temperature controller.

### 3. Results and discussion

As shown in Fig. 1(b), the dielectric layer showed a very smooth surface with a roughness  $< 5$  nm. This enables us to grow the semiconductor ( $\text{C}_{60}$ ) with a very good control of the film morphology (Fig. 1(c)). A recent study shows that the first couple of monolayers next to the dielectric dominates the charge transport in organic semiconductor layers [17].

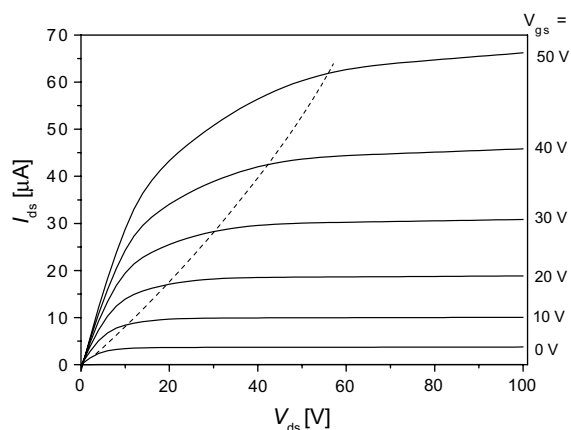


Fig. 2.  $I_{\text{ds}}(V_{\text{ds}})$  curve of the OFET in the accumulation mode. The dotted line is a guide for the eye for saturated  $I_{\text{ds}}$ . The data shown here are taken in ascending  $V_{\text{gs}}$  mode with an integration time of 1 s.

Fig. 2 shows the transistor characteristics of a device with a well saturated curve occurring pinch off at a drain source voltage  $V_{\text{ds}} \geq V_{\text{gs}}$  (gate voltage). From the slope at  $V_{\text{ds}} = 0$  V of the curve at  $V_{\text{gs}} = 0$  V, we estimated a conductivity of  $5 \times 10^{-6}$  S cm<sup>-1</sup>. For the same device (see Fig. 3) we measured the transfer characteristics. The data presented in Fig. 3 hold for  $V_{\text{ds}} = 60$  V. One can

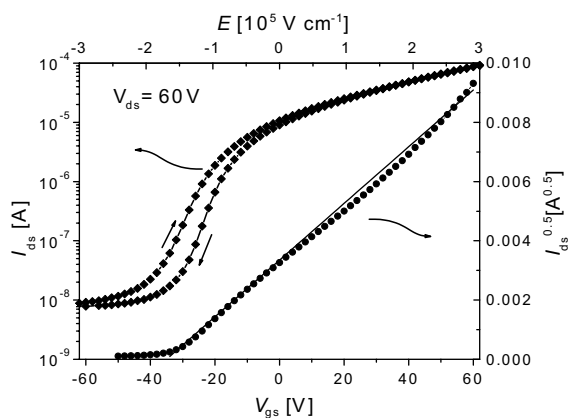


Fig. 3. Semilogarithmic plot of  $I_{\text{ds}}$  vs.  $V_{\text{gs}}$  (left scale) and plot of  $I_{\text{ds}}^{0.5}$  vs  $V_{\text{gs}}$  (right scale) for the same  $\text{C}_{60}$  OFET as in Fig. 2. The full line shows a fit to the data (return curve) using Eq. (1) from which a field-effect mobility  $\mu = 0.63$  cm<sup>2</sup>/Vs is obtained. Each measurement was carried out with an integration time of 1 s.

see that the transistor turns on at an onset voltage of  $V_t = -35$  V without significant hysteresis and the drain–source current  $I_{ds}$  increases quadratically. The device shows an on/off ratio  $> 10^4$  which is calculated as the ratio of  $I_{ds}$  at  $V_{gs} = 60$  V and  $I_{ds}$  at  $V_{gs} = V_t$ . We have observed consistently the effect of having large drain–source current even when  $V_{gs} = 0$  V. This effect is minimized when the dielectric layer is preheated at high temperature prior to the deposition of the active layer. This effect is proposed to be due to the presence of unintentional dopants at the interface of the untreated dielectric. Interfacial effects seem to play a major role in organic electronics devices [18]. From  $V_t = -(qn_0d_sC_{BCB}) + V_{fb}$ , [19] where  $V_{fb} = 0.1$  V [16] is the flat band potential (which accounts for the work function difference between the semiconductor and the gate electrode without considering fixed charges at the dielectric and at the interface),  $d_s$  is the thickness of the semiconductor,  $q$  is the elementary charge and  $C_{BCB}$  is the capacitance of the gate dielectric, we were able to estimate the density of free carriers at equilibrium  $n_0$ . This yields a relatively high electron density of  $\sim 10^{17}$  cm $^{-3}$ .

As shown in Fig. 3, from the fit to the data using equation [20]:

$$I_{ds} = \frac{\mu WC_{BCD}}{2L} (V_{gs} - V_t)^2 \quad (1)$$

we extract a field effect mobility of  $0.63$  cm $^2$ V $^{-1}$ s $^{-1}$  in the saturation regime for  $V_{ds} = 60$  V (note the fitting line used for the mobility extraction fits the data over a wide range of  $V_{gs}$ ). However, for calculating the field effect mobility, the contact resistance of LiF/Al and C $_{60}$  is not taken into account by assuming that the contact resistance is fairly low. Our studies of the dependence of the field effect mobility on the metal work function in soluble methanofullerene based OFETs have shown a highest obtained mobility  $\mu$  of  $0.2$  cm $^2$ V $^{-1}$ s $^{-1}$  with LiF/Al as drain–source electrode. Use of higher work function metal electrodes viz. Cr, Au, etc. in these OFETs leads to slightly reduced mobilities presumably due to large contact resistance [18]. Similarly we have also observed a slight decrease in the field effect mobility in C $_{60}$  OFETs with higher work function electrodes (not shown here). The

device performance and the mobility strongly depends on the choice of the dielectric layer mainly due to the different surface energies of dielectric layers. The sharp turn on of  $I_{ds}$  is a measure of the quality of the dielectric/semiconductor interface which is defined by the normalized subthreshold slope,  $S = C_{BCB}dV_{gs}/d(\log I_{ds})$  [5]. As usually observed in organic FETs, a subthreshold slope of  $8$  VnF/decadecm $^2$  obtained by us is very high which can be reduced by reducing the thickness of the dielectric layer. We presume, the most important factor in achieving this high mobility OFET is the combination of a smooth organic dielectric surface with a highly ordered C $_{60}$  film grown by HWE [13]. It can be mentioned here that very few studies have been done so far on growing highly ordered organic thin films on top of organic dielectrics partly due to low glass transition temperatures and unwanted hysteresis. Use of BCB among other organic dielectrics is based on the fact that it provides devices with a small hysteresis. In addition BCB is a high glass transition temperature polymer, an additional advantage for optimizing the film growth conditions at high substrate temperatures. Previous reports on C $_{60}$  FETs grown on SiO $_2$  have shown highest obtained mobilities of  $0.5$  cm $^2$ V $^{-1}$ s $^{-1}$  [6e].

We further analysed the validity of Eq. (1) for different  $V_{ds}$  via local approximation assuming  $V_{gs}$  independent of  $\mu$ :

$$\mu = \frac{2L}{WC_{BCD}} \left( \frac{\partial \sqrt{I_{ds}}}{\partial V_{gs}} \right)^2 \quad (2)$$

The mobility as a function of  $V_{gs}$  was determined assuming Eq. (2), which is valid in the saturation regime, at  $V_{ds} = 60$  V. As shown in Fig. 4 the mobility is found to be almost constant for  $V_{ds} \geq 123V_{gs}$  with values as high as  $1$  cm $^2$ /Vs at  $V_{gs}, V_{ds} = 60$  V. These mobilities are comparable with the electron mobility determined by photocurrent measurements [21] or time of flight experiment on single crystalline C $_{60}$  [22]. Further we carried out measurements at very large  $V_{gs}$  (up to  $100$  V) and very large  $V_{ds}$  (up to  $100$  V) where we observed a non-linear transport which leads to a trap filled limited (TFL) regime [23]. We have observed a drastic increase in the device perfor-

mance and its field-effect mobility in the devices when the dielectric layer is cleaned by preheating in situ at temperatures above 250 °C which normally occurs during the epitaxial growth of thin films [23]. The values shown here are an average of at least fifty different devices fabricated under identical conditions with a narrow statistical distribution in the obtained mobility. We also calculated the transconductance,  $g = (\partial V_{gs}/\partial I_{ds})$  [20] of these devices and plotted the channel resistance  $g^{-1}$  vs.  $V_{gs}$  in Fig. 4. We observed a  $g$  in the range of 3–10  $\mu\text{S}$  which is again a relatively high value for an n-type organic semiconductor.

Loading of the devices in a cryostat for low temperature studies was done by carefully loading the devices inside the glove box environment. Such an arrangement is in general needed in order not to degrade the device performance which normally occurs in *n*-channel OFETs during transportation. C<sub>60</sub> OFETs exhibit a temperature dependent mobility with an Arrhenius behaviour as shown in Fig. 5. The activation energy obtained is  $\sim 100$  meV. This activation energy may be influenced by several parameters including a temperature dependent contact resistance. An activation energy of the same order is also found in soluble methanofullerene based OFETs while it is difficult to state what really causes the activation energy in these devices [18].

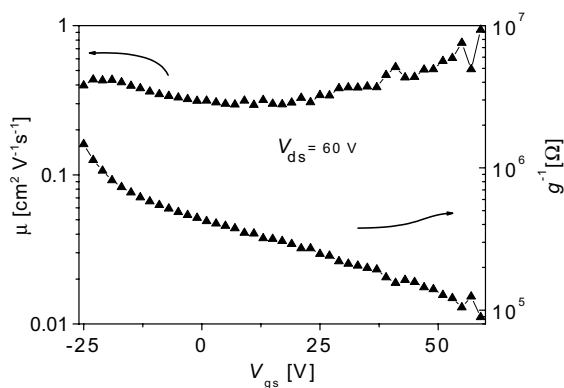


Fig. 4. Effective FET mobility (left scale) obtained from the channel transconductance after Eq. (2) showing a step-wise dependence on  $V_{gs}$  with a nearly constant  $\mu$  over a large range of  $V_{gs}$  in the saturated regime ( $V_{ds} = 60$  V). Channel resistance  $1/g$  (right scale) as a function of  $V_{gs}$ .

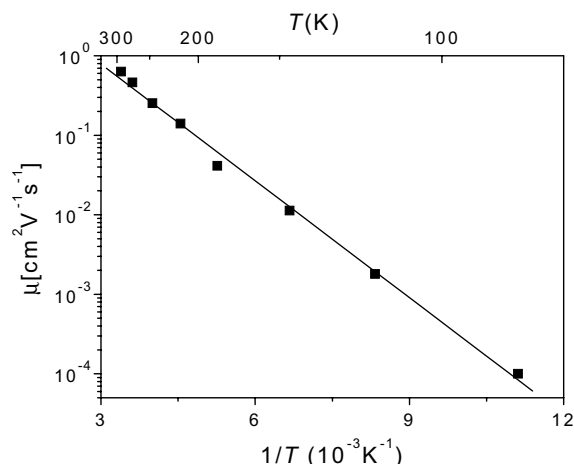


Fig. 5. Arrhenius plot of the temperature dependent mobility of C<sub>60</sub> BCB OFETs.

#### 4. Conclusions

In conclusion, we have demonstrated an *n*-channel OFET with an electron mobility of 0.4–1  $\text{cm}^2\text{V}^{-1}\text{s}^{-1}$  along with an on/off ratio  $>10^4$  using a solution based organic dielectric BCB film in combination with HWE grown C<sub>60</sub> films. The obtained mobility is nearly gate voltage independent.

#### Acknowledgements

Special thanks are to Michael Auinger and Philipp Stadler for technical help. This work was performed within the Christian Doppler Society's dedicated laboratory on Plastic Solar Cells funded by the Christian Doppler Society and Konarka Austria GesmbH. Furthermore, we acknowledge financial support from the Austrian Foundation for the Advancement of Scientific Research (FWF P15155, P15627 and P15629).

#### References

- [1] (a) Two most recent review articles, W. Clemens, W. Fix, J. Ficker, A. Knobloch, A. Ullmann, J. Mater. Res. 19 (2004) 1963;

- (b) G. Horowitz, J. Mater. Res. 19 (2004) 1946, and references therein.
- [2] B. Crone, A. Dodabalapur, Y.-Y. Lin, R.W. Filas, Z. Bao, A. Laduca, R. Sarpeshkar, H.E. Katz, W. Li, Nature 403 (2000) 521.
- [3] H.E.A. Huitema, G.H. Gelinck, J.B.P.H. van der Putten, K.E. Kuijk, C.M. Hart, E. Cantatore, P.T. Herwig, A.J.J.M. van Breemen, D.M. de Leeuw, Nature 414 (2001) 599.
- [4] J.A. Rogers, Z. Bao, K. Baldwin, A. Dodabalapur, B. Crone, V.R. Raju, V. Kuck, H.E. Katz, K. Amundson, J. Ewing, P. Drzaic, Proc. Natl. Acad. Sci. 98 (2001) 4835.
- [5] (a) Y.-Y. Lin, D.J. Gundlach, S.F. Nelson, T.N. Jackson, IEEE Electr. Dev. Lett. 18 (1997) 606;  
(b) V.C. Sundar, J. Zaumseil, V. Podzorov, E. Menard, R.L. Willett, T. Someya, M.E. Gershenson, J.A. Rogers, Science 303 (2004) 1644.
- [6] (a) J. Kastner, J. Paloheimo, H. Kuzmany, in: H. Kuzmany, M. Mehring, J. Fink (Eds.), Electronic Properties of High- $T_c$  Superconductors, Springer Series in Solid State Sciences, 1993;  
(b) R.C. Haddon, A.S. Perel, R.C. Morris, T.T.M. Palstra, A.F. Hebard, Appl. Phys. Lett. 67 (1995) 121;  
(c) R.C. Haddon, J. Am. Chem. Soc. 118 (1996) 3041;  
(d) K. Horiuchi, K. Nakada, S. Uchino, S. Hashii, A. Hashimoto, N. Aoki, Y. Ochiai, M. Shimizu, Appl. Phys. Lett. 81 (2002) 1911;  
(e) S. Kobayashi, T. Takenobu, S. Mori, A. Fujiwara, Y. Iwasa, Appl. Phys. Lett. 82 (2003) 4581;  
(f) S. Kaboyashi, S. Mori, S. Lida, H. Ando, T. Takenobu, Y. Taguchi, A. Fujiwara, A. Taninaka, H. Shinohara, Y. Iwasa, J. Am. Chem. Soc. 125 (2003) 8116.
- [7] (a) K. Shibata, Y. Kubozono, T. Kanabara, T. Hosokawa, T. Hosokawa, A. Fuziwara, Y. Ito, H. Shinohara, Appl. Phys. Lett. 84 (2004) 2572;  
(b) T. Kanabara, K. Shibata, S. Fujiki, Y. Kubozono, S. Kashino, Y. Kubozono, S. Kashino, T. Urisu, M. Sakai, A. Fujiwara, R. Kumashiro, K. Tanigaki, Chem. Phys. Lett. 379 (2003) 223.
- [8] Z. Bao, A.J. Lovinger, J. Brown, J. Am. Chem. Soc. 120 (1998) 207.
- [9] H.E. Katz, J. Johnson, A.J. Lovinger, W. Li, J. Am. Chem. Soc. 122 (2000) 7787.
- [10] R.J. Chesterfield, J.C. McKeen, Ch.R. Newman, C.D. Frisbie, P.C. Ewbank, K.R. Mann, L.L. Miller, J. Appl. Phys. 95 (2004) 6396.
- [11] P.R.L. Malenfant, C.D. Dimitrakopoulos, J.D. Gelorme, L.L. Kosbar, T.O. Graham, Appl. Phys. Lett. 80 (2002) 2517.
- [12] A. Andreev, G. Matt, C.J. Brabec, H. Sitter, D. Badt, H. Seyringer, N.S. Sariciftci, Adv. Mater. 12 (2000) 629.
- [13] D. Stifter, H. Sitter, Appl. Phys. Lett. 66 (1995) 679.
- [14] L.-L. Chua, P.K.H. Ho, H. Sirringhaus, R.H. Friend, Appl. Phys. Lett. 84 (2004) 3400.
- [15] R. Schwödiauer, G.S. Neugschwandtner, S. Bauer-Gogonea, S. Bauer, W. Wirges, Appl. Phys. Lett. 75 (1999) 3998.
- [16] (a) V.D. Mihailetschi, J.K.J. van Duren, P.W.M. Blom, J.C. Hummelen, R.A.J. Janssen, J.M. Kroon, M.T. Rispens, W.J.H. Verhees, M.M. Wienk, Adv. Funct. Mater. 13 (2003) 43;  
(b) G.J. Matt, N.S. Sariciftci, T. Fromherz, Appl. Phys. Lett. 84 (2004) 1570;  
(c) C.J. Brabec, A. Cravino, D. Meissner, N.S. Sariciftci, T. Fromherz, M.T. Rispens, L. Sanchez, J.C. Hummelen, Adv. Funct. Mater. 11 (2001) 374.
- [17] F. Dinelli, M. Murgia, P. Levy, M. Cavallini, F. Biscarini, D.M. de Leeuw, Phys. Rev. Lett. 92 (2004) 116802.
- [18] Th.B. Singh, N. Marjanović, Ph. Stadler, M. Auinger, G.J. Matt, S. Günes, N.S. Sariciftci, R. Schwödiauer, S. Bauer, J. Appl. Phys. 97 (2005) 083714.
- [19] G. Horowitz, R. Hajlaoui, F. Kouki, Eur. Phys. J. AP 1 (1998) 361.
- [20] S.M. Sze, Physics of Semiconductor Devices, Wiley, New York, 1981;  
M. Shur, M. Hack, J. Appl. Phys. 55 (1984) 3831.
- [21] D. Sarkar, N.J. Halas, Solid State Commun. 90 (1994) 261.
- [22] E. Frankevich, Y. Maruyama, H. Ogata, Chem. Phys. Lett. 214 (1993) 39.
- [23] Th. B. Singh, N. Marjanović, G.J. Matt, S. Günes, Ph. Stadler, M. Auinger, N.S. Sariciftci, R. Schwödiauer, S. Bauer, A. Montaigne Ramil, A. Andreev, H. Sitter, submitted.